0026-895X/06/6901-354–362$20.00
MOLECULAR PHARMACOLOGY
Copyright © 2006 The American Society for Pharmacology and Experimental Therapeutics
Mol Pharmacol 69:354–362, 2006

Vol. 69, No. 1
17210/3073431
Printed in U.S.A.

Pharmacological Profiling of *Orthochirus scrobiculosus* Toxin 1 Analogs with a Trimmed N-Terminal Domain

Stéphanie Mouhat, Georgeta Teodorescu, Daniel Homerick, Violeta Visan, Heike Wulff, Yingliang Wu, Stephan Grissmer, Hervé Darbon, Michel De Waard, and Jean-Marc Sabatier

Laboratoire Cellpep S.A., Marseille, France; Centre National de la Recherche Scientifique Formation de Recherche en Evolution 2738, Marseille, France (S.M., J.-M.S.); Universität Ulm, Ulm, Germany (G.T., V.V., S.G.); Department of Medical Pharmacology and Toxicology, University of California, Davis, Davis, California (D.H., H.W.); College of Life Sciences, Wuhan University, Wuhan, China (Y.W.); AFMB, Centre National de la Recherche Scientifique UPR 9039, Marseille, France (H.D.); Institut National de la Santé et de la Recherche Médicale U607, Département Réponse Dynamique et Cellulaire, Grenoble, France; CEA, Grenoble, France; and Université Joseph Fourier, Grenoble, France (M.D.W.)

Received July 25, 2005; accepted October 18, 2005

ABSTRACT

OSK1, a toxin from the venom of the Asian scorpion *Orthochirus scrobiculosus*, is a 38-residue peptide cross-linked by three disulfide bridges. A structural analog of OSK1, [Lys^{16},Asp^{20}]-OSK1, was found previously to be one of the most potent blockers of the voltage-gated K^+ channel Kv1.3 hitherto characterized. Here, we demonstrate that progressive trimming of the N-terminal domain of [Lys^{16},Asp^{20}]-OSK1 results in marked changes in its pharmacological profile, in terms of both K^+ channel affinity and selectivity. Whereas the affinity to Kv1.1 and Kv1.3 did not change significantly, the affinity to Kv1.2 and K_{Ca}3.1 was drastically reduced with the truncations. It is surprising that a striking gain in potency was observed for Kv3.2. In contrast, a truncation of the C-terminal domain, expected to partially disrupt the toxin β-sheet structure, resulted in a significant decrease or a complete loss of activity on all channel types tested. These data highlight the value of structure-function studies on the extended N-terminal domain of [Lys^{16},Asp^{20}]-OSK1 to identify new analogs with unique pharmacological properties.

OSK1 is a toxin that originates from the venom of the Asian scorpion *Orthochirus scrobiculosus* (Jaravine et al., 1997). It is composed of 38 amino acid residues with three disulfide bridges that are arranged according to a conventional pattern of the type C1–C4, C2–C5, and C3–C6 (Jaravine et al., 1997; Mouhat et al., 2004a,b). OSK1, also referred to as α-KTx3.7, belongs to the α-KTx3 family (Tytgat et al., 1999; Rodriguez de la Vega and Possani, 2004) and shares between 74 and 90% sequence identity with other members of this family, such as kaliotoxin 1 (Aiyar et al., 1995), agitoxins 1, 2, and 3 (Garcia et al., 1994), and *Buthus martensi* kaliotoxin-like BmkTX (Romi-Lebrun et al., 1997). The 3-D solution structure of OSK1, as determined by ^{1}H NMR (Protein Data Bank accession code 1SCO), indicates that the toxin folds according to the canonical α/β architectural motif, which corresponds to a helical structure connected to an antiparallel β-sheet by two disulfide bridges (Bontems et al., 1991; Jaravine et al., 1997; Mouhat et al., 2004b). In the case of OSK1, the helical structure is a distorted α-helix running from amino acid residues 10 to 21, whereas the antiparallel β-sheet is composed of two strands going from residues 24 to 28 and 32 to 38. The N-terminal domain contains an ex-

Article, publication date, and citation information can be found at http://molpharm.aspetjournals.org.
doi:10.1124/mol.105.017210.

ABBREVIATIONS: OSK1, toxin 1 from the scorpion *Orthochirus scrobiculosus*; AOSK1, [Lys^{16},Asp^{20}]-OSK1; [Δ^1]-AOSK1, AOSK1 deleted of the amino acid residue at position 1; [Δ^{1-4}]-AOSK1, AOSK1 deleted of the four N-terminal residues; [Δ^{1-6}]-AOSK1, AOSK1 deleted of the six N-terminal residues; [Δ^{1-7}]-AOSK1, AOSK1 deleted of the seven N-terminal residues; [Δ^{36-38}]-AOSK1, AOSK1 deleted of the last three C-terminal residues; [Δ^1,Thr^2]-AOSK1, AOSK1 deleted of the amino acid residue at position 1 and mutated at position 2 by a threonine residue; Fmoc, *N*α-fluoren-9-ylmethyloxycarbonyl; TFA, trifluoroacetic acid; HPLC, high-performance liquid chromatography; Kv, mammalian voltage-gated K^+ channels (Kv1.1 to Kv1.7); K_{Ca}2.1 (also referred to as SK1), type-1 small-conductance Ca^{2+}-activated K^+ channel; K_{Ca}2.2 (also referred to as SK2), type 2 small-conductance Ca^{2+}-activated K^+ channel; K_{Ca}3.1 (also referred to as IK1), type 1 intermediate-conductance Ca^{2+}-activated K^+ channels; K_{Ca}1.1 (also referred to as BK), large-conductance Ca^{2+}-activated K^+ channel; Kv11.1 (also referred to as HERG), human *ether-a-go-go*-related K^+ channel; HEK, human embryonic kidney.

a

b

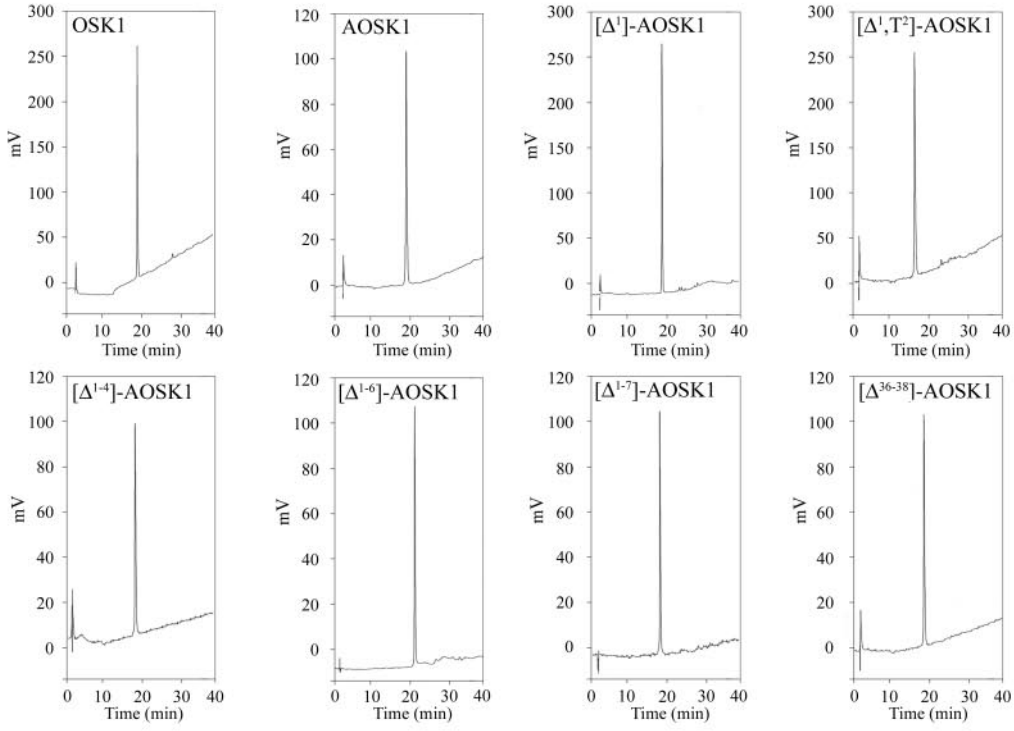

c

Peptide	Deduced Mr $(M+H)^+$	Experimental Mr $(M+H)^+$
OSK1	4206.2	4206.6
AOSK1	4192.2	4193.0
$[\Delta^1]$-AOSK1	4135.2	4135.6
$[\Delta^{1,}T^2]$-AOSK1	4137.1	4137.4
$[\Delta^{1-4}]$-AOSK1	3809.7	3809.9
$[\Delta^{1-6}]$-AOSK1	3596.5	3596.9
$[\Delta^{1-7}]$-AOSK1	3468.3	3468.7
$[\Delta^{36-38}]$-AOSK1	3865.8	3866.5

tended structure (residues 2–6) resembling a third strand of the β-sheet.

OSK1 is a potent blocker of Kv1-family potassium channels that targets Kv1.1 (IC_{50} = 0.6 nM for current block), Kv1.2 (IC_{50} = 5.4 nM), and Kv1.3 (IC_{50} =14 pM) with picomolar-to-nanomolar affinity. It is also moderately active on the calcium-activated K^+ channel $K_{Ca}3.1$ (IC_{50} = 225 nM) (Mouhat et al., 2004b). Because OSK1 blocks both Kv1.3 and $K_{Ca}3.1$, two channels involved in the activation of human T and B cells (Chandy et al., 2004; Wulff et al., 2004), it constitutes a good lead compound for the development of new, OSK1-derived immunosuppressive peptides of therapeutic value. We have reported the design and chemical production of an OSK1 analog, [Lys^{16},Asp^{20}]-OSK1 (here referred to as AOSK1), that is approximately five times more potent on Kv1.3 (IC_{50} = 3 pM) than OSK1 itself (Mouhat et al., 2004b). As such, AOSK1 is one of the most potent Kv1.3 channel blockers characterized so far. AOSK1 blocks $K_{Ca}3.1$ with roughly the same affinity as OSK1 itself, but it displays a higher selectivity over Kv1.1 and Kv1.2. Here, this analog was used as a template for the production and pharmacological characterization of a number of novel OSK1 analogs. Trimming of the N-terminal extended domain of AOSK1 specifically reduced the affinity for Kv1.2 and $K_{Ca}3.1$ but did not significantly change the affinity for Kv1.1 and Kv1.3. Partial sequence trimming also proved to be an unexpected and powerful approach to obtain AOSK1 analogs with pharmacological activities toward new K^+ channel subtypes such as Kv3.2.

Materials and Methods

Materials. Fmoc-L-amino acids, 4-hydroxymethylphenyloxy resin, and reagents used for peptide synthesis were obtained from PerkinElmer Life and Analytical Sciences (Boston, MA). Solvents were analytical grade products from SDS (Witham, Essex, UK). L929, B82, and MEL cells stably expressing rat Kv1.2, mouse Kv1.3, human Kv1.5, and mouse Kv3.1 have been described previously (Grissmer et al., 1994). Cells lacking leukocyte tyrosine kinase (LTK cells) expressing human Kv1.4 were obtained from Professor Michael Tamkun (Colorado State University, Fort Collins, CO), Chinese hamster ovary cells expressing mouse Kv1.7 were from Vertex Pharmaceuticals (San Diego, CA). Human embryonic kidney (HEK) 293 cells expressing human $K_{Ca}1.1$ were from Dr. Andrew Tinker (Centre for Clinical Pharmacology, University College London, London, UK); HEK 293 cells expressing human Kv11.1 (HERG) channel were from Professor Craig T. January (Department of Medicine, University of Wisconsin, Madison, WI); and HEK 293 cells expressing human $K_{Ca}2.1$ and $K_{Ca}3.1$ were from Dr. Khaled Houamed (University of Chicago, Chicago, IL).

Production of AOSK1 Analogs by Solid-Phase Peptide Synthesis. AOSK1 was obtained as described previously (Mouhat et al., 2004b). The AOSK1 analogs ([Δ^1]-AOSK1, [Δ^{1-4}]-AOSK1, [Δ^{1-6}]-AOSK1, [Δ^{1-7}]-AOSK1, [Δ^{36-38}]-AOSK1, and [Δ^1, Thr^2]-AOSK1) were produced by chemical synthesis using a peptide synthesizer (model 433A; Applied Biosystems, Foster City, CA). Peptide chains were assembled stepwise on 0.25 mmol 4-hydroxymethylphenyloxy resin (1% cross-linked; 0.65 mmol of amino group per gram) using 1 mmol Fmoc-L-amino acid derivatives (Merrifield, 1986). Side chain-protecting groups for trifunctional residues were trityl for cysteine, asparagine, histidine, and glutamine; *t*-butyl for serine, threonine, tyrosine, aspartate, and glutamate; 2,2,4,6,7-pentamethyldihydrobenzofuran-5-sulfonyl for arginine; and *t*-butyloxycarbonyl for lysine. N^{α}-amino groups were deprotected by successively treating with 18 and 20% (v/v) piperidine/*N*-methylpyrrolidone for 3 and 8 min, respectively. After three washes with *N*-methylpyrrolidone, the Fmoc-amino acid derivatives were coupled (20 min) as their hydroxybenzotriazole active esters in *N*-methylpyrrolidone (4-fold excess). After peptides were assembled, and removal of N-terminal Fmoc groups, the peptide resins (approximately 1.5 g) were treated under stirring for 3 h at 25°C with mixtures of TFA/H_2O/thioanisole/ethanedithiol (73:11:11:5, v/v) in the presence of crystalline phenol (2.1 g) in final volumes of 30 ml per gram of peptide resins. The peptide mixtures were filtered, precipitated, and washed twice with cold diethyloxide. The crude peptides were pelleted by centrifugation (3200*g* for 8 min). They were then dissolved in H_2O and freeze-dried. Reduced AOSK1 analogs were solubilized at a concentration of approximately 0.6 mM in 0.2 M Tris-HCl buffer, pH 8.3, for oxidative folding (40–120 h depending on the peptide, 20°C). The folded/oxidized peptides were purified to homogeneity by reverse-phase high-performance liquid chromatography (HPLC) (C_{18} Aquapore ODS, 20 μm, 250 × 10 mm; PerkinElmer) by means of a 60-min linear gradient of 0.10% (v/v) TFA/H_2O (buffer A) with 0 to 40% of 0.08% (v/v) TFA/acetonitrile (buffer B) at a flow rate of 6 ml/min (λ = 230 nm). The purity and identity of each peptide were assessed by 1) analytical C_{18} reverse-phase HPLC (C_{18} Lichrospher 5 μm, 4 × 200 mm; Merck, Darmstadt, Germany) using a 40-min linear gradient of buffer A with 0 to 60% of buffer B at a flow rate of 1 ml/min; 2) amino acid analysis after peptide acidolysis [6 M HCl/2% (w/v) phenol, 20 h, 120°C, N_2 atmosphere]; and 3) molecular mass determination by matrix-assisted laser-desorption ionization-time-of-flight spectrometry.

Conformational Analyses of AOSK1 Analogs by One-Dimensional ^{1}H NMR. AOSK1 analogs were dissolved in a 9/1 mixture of H_2O/D_2O (v/v) at final concentrations of 50 μM. All ^{1}H NMR measurements were performed on a Bruker DRX 500 spectrometer equipped with an HCN probe (Bruker, Newark, DE), and self-shielded triple axis gradients were used. Experiments were performed at 300 K.

Lethality of AOSK1 Analogs in Mice. The peptides were evaluated for toxicity in vivo by determining the LD_{50} value after intracerebroventricular injection into 20-g C57/BL6 mice (approved by the French ethics committee; animal testing agreement number 13.231 delivered by the Direction Départementale des Services Vétérinaires des Bouches-du-Rhône, Préfecture des Bouches-du-Rhône, France). Groups of six to eight mice per dose were injected with 5 μl of peptide solution containing 0.1% (w/v) bovine serum albumin and 0.9% (w/v) NaCl.

Cell Cultures and Transfections. B82, MEL, L929, and HEK cells stably expressing the above-mentioned voltage- and Ca^{2+}-activated K^+ channels and COS-7 cells used for transfection were maintained in Dulbecco's modified Eagle's medium with Earle's salts (Invitrogen, Carlsbad, CA), and 10% heat-inactivated fetal calf serum (PAA Laboratories GmbH, Linz, Austria) as described previously (Grissmer et al., 1994). Mouse Kv1.1 in a GFPIre vector (Invitrogen), human Kv1.2 in a pcDNA3/Hygro vector (Invitrogen), and rat Kv3.2 in a pcDNA3 vector (Protinac GmbH, Hamburg, Germany) were transfected into COS-7 cells either alone or with a green fluo-

Fig. 1. Amino acid sequences and chemical syntheses of OSK1, AOSK1, and analogs thereof. a, the amino acid sequences (one-letter code) of OSK1, AOSK1, and AOSK1 analogs were aligned according to the positions of their half-cystine residues (numbered from 1 to 6). The positions of half-cystine residues are highlighted in gray boxes. Mutated residues in AOSK1 (Lys^{16} and Asp^{20}) and related analogs are shown in boldface type. The positions of OSK1 secondary structures (an N-terminal extended domain located before the first half-cystine residue, an α-helix, and a two-stranded β-sheet structure) are indicated by solid lines above the toxin amino acid sequence (1). The 3-D solution structure of OSK1 can be found in the Protein Data Bank (code 1SCO). b, analytical C_{18} reverse-phase HPLC elution profiles of folded/oxidized OSK1, AOSK1, and its N- or C-terminal truncated analogs after their purification steps. c, deduced and experimental relative molecular masses $(M+H)^+$ of synthetic OSK1, AOSK1, and its analogs.

rescent protein-expressing construct using FuGene6 Transfection Reagent (Roche Diagnostics, Mannheim, Germany) according to the recommended protocol. Currents were recorded 1 to 3 days later in green fluorescent protein-positive cells.

Electrophysiology. Electrophysiological experiments were carried out at 22 to 24°C using the patch-clamp whole-cell recording mode (Hamill et al., 1981; Rauer and Grissmer, 1996). Cells were bathed with mammalian Ringer's solution: 160 mM NaCl, 4.5 mM KCl, 2 mM $CaCl_2$, 1 mM $MgCl_2$, and 10 mM HEPES, pH 7.4 with NaOH, with an osmolarity of 290 to 320 mOsM. When AOSK1 analogs were applied, 0.1% bovine serum albumin was added to the Ringer's solution. A syringe-driven perfusion device was used to exchange the external recording bath solution. Two internal pipette solutions were used: one for measuring voltage-gated K^+ currents that contained 155 mM KF, 2 mM $MgCl_2$, 10 mM HEPES, and 10 mM EGTA, pH 7.2 with KOH, with an osmolarity of 290 to 320 mOsM; the other was for measuring Ca^{2+}-activated K^+ currents that contained 135 mM potassium aspartate, 8.7 mM $CaCl_2$, 2 mM $MgCl_2$, 10 mM EGTA, and 10 mM HEPES, pH 7.2 with KOH, with an osmolarity of 290 to 320 mOsM. A free $[Ca^{2+}]_i$ value of 1 μM was calculated. All currents through voltage-gated K^+ channels were elicited by 200-ms depolarizing voltage steps from −80 to +40 mV. Potassium currents through $K_{Ca}1.1$, $K_{Ca}2.1$, and $K_{Ca}3.1$ were elicited by 1 μM internal $[Ca^{2+}]_i$ and 200-ms voltage ramps from −120 to +40 mV. Electrodes were pulled from glass capillaries (Science Products, GmbH, Hofheim, Germany) and fire-polished to resistances of 2.5 to 5 MΩ. Membrane currents were measured with an EPC-9 or EPC-10 patch-clamp amplifier (HEKA Elektronik, Lambrecht/Pfalz, Germany) interfaced to a computer running acquisition and analysis software (Pulse and PulseFit). When voltage-gated K^+ currents were measured, the capacitive and leak currents were subtracted using a P/10 procedure. Series resistance compensation (>80%) was used for currents greater than 2 nA. The holding potential was −80 mV in all experiments. Data analyses were performed with IgorPro (WaveMetrics, Lake Oswego, OR), and IC_{50} values were deduced by fitting a modified Hill equation to the data ($I_{toxin}/I_{control} = 1/[1 + ([AOSK1\ analog]/IC_{50})]$, where I is the peak current (for voltage-gated K^+ channels) or the slope of the ramp current (for Ca^{2+}-activated K^+ channels) to the normalized data points obtained with at least four different AOSK1 analog concentrations.

Results

Syntheses of AOSK1 Analogs. A comparison of the amino acid sequences of OSK1, AOSK1, and its analogs is provided in Fig. 1a. AOSK1 is an OSK1 analog with two mutations in positions 16 (acidic Glu^{16} replaced by basic lysine) and 20 (basic Lys^{20} replaced by acidic aspartic acid). Although the net global charge of AOSK1 is the same as that of OSK1, the distribution of charged amino acid residues is different between the two compounds. A previous study dem-

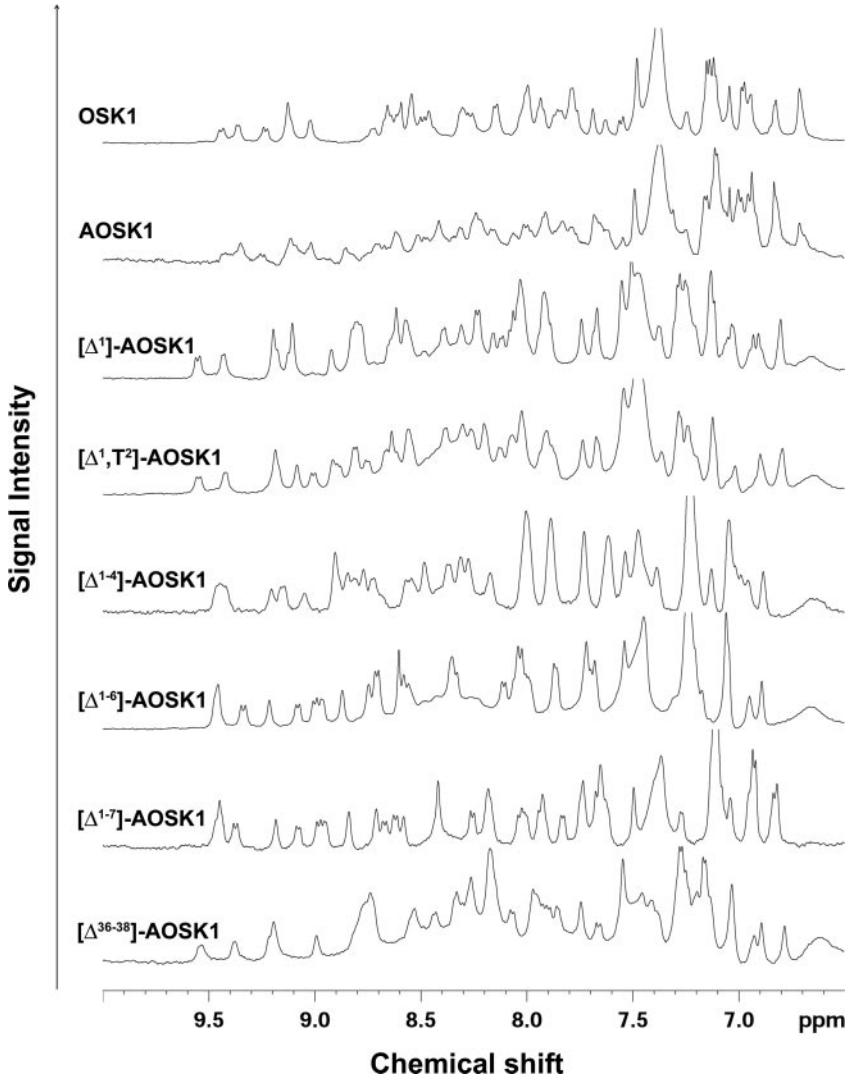

Fig. 2. Structural analysis of AOSK1 peptides by ^1H NMR. One-dimensional ^1H NMR spectra of AOSK1 and its truncated analogs. The spectrum of OSK1 is shown for comparison. Only the representative amide proton regions are shown. The overall distribution of resonance frequencies suggests that all peptides have similar global folds.

onstrated that AOSK1 is a 5-fold more potent blocker of Kv1.3 than is OSK1 (Mouhat et al., 2004b). AOSK1 is also more selective for Kv1.3 than OSK1. We therefore used it as a template for the rationale design of new structural analogs in which we trimmed either the N or C terminus. In both cases, the number and relative positioning of all six half-cystine residues forming the three-disulfide bridges were preserved. The standard structural motif for the α/β scaffold in most scorpion toxins can be described by $\mathbf{X}_n CX_n CX_3 CX_n$-(G/A/S)$XCX_n CXC\mathbf{X}_n$ (where X represents an unspecified amino acid residue and n a variable number of residues). Boldface $\mathbf{X}_n$ at N- and C-terminal extremities represent the residues that were selectively trimmed in the design of AOSK1 analogs. Using this approach, four N-terminal truncated AOSK1 analogs ([Δ^1]-AOSK1, [Δ^{1-4}]-AOSK1, [Δ^{1-6}]-AOSK1, and [Δ^{1-7}]-AOSK1) were chemically produced that shortened the N-terminal extended domain but kept the first AOSK1 half-cystine residue intact. We further synthesized an analog in which we truncated the first N-terminal amino acid residue (Gly^1) and mutated the second amino acid residue of AOSK1 from Val^2 to threonine ([Δ^1,Thr^2]-AOSK1). This point mutation was selected to produce an AOSK1 analog possessing an N-terminal domain (i.e., TIINVK) that is identical with those of margatoxin and noxiustoxin, two scorpion toxins that potently block Kv1.3 (Possani et al., 1999; Rodriguez de la Vega et al., 2003). In addition, a C-terminal-truncated AOSK1 analog ([Δ^{36-38}]-AOSK1) was synthesized to evaluate the importance of this domain. The latter truncates half of the second strand (amino acid sequence 32–38) of the β-sheet structure, and we therefore expected it to show a reduced potency because of the reported importance of the β-sheet structure for Kv channel blockage (Regaya et al., 2004). All of the peptides were assembled by solid-phase synthesis using stepwise Fmoc/*t*-butyl chemistry, as described previously (Merrifield, 1986). After assembly, crude reduced peptides were obtained in yields ranging from 70 to 80%. The peptides were folded/oxidized under standard alkaline conditions and purified by preparative C_{18} reverse-phase HPLC. Homogeneity of the purified peptides was >99%, as assessed by analytical HPLC (Fig. 1b). Mass spectrometry analyses of the peptides using the matrix-assisted laser-desorption ionization-time-of-flight technique gave experimental molecular masses similar to the deduced molecular masses (Fig. 1c), validating the identity of the desired products. All peptides were also characterized and quantified by amino acid analyses after acidolysis. A complete Edman sequencing was performed for some of them to further validate the final products (data not shown). The yield of peptide synthesis ranged between 1 and 5%.

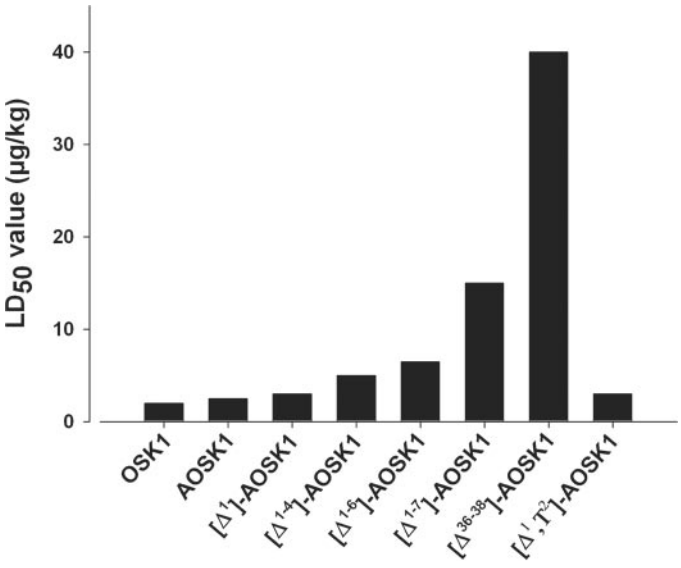

Fig. 3. Lethal activities of AOSK1 and its analogs in vivo in mice. LD_{50} values are provided in micrograms of peptide per kilogram of mouse. The LD_{50} value of OSK1 is indicated for comparison.

Structural Analysis of AOSK1 and Truncated Analogs by ^{1}H NMR. One-dimensional ^{1}H NMR was used to verify that the truncations did not generate unfolded species (Fig. 2). The well-dispersed signals of the amide regions suggest that the AOSK1 analogs are folded in compact conformations.

Comparison of Lethal Activities between AOSK1 and Its Analogs in Mice. The synthetic peptides were compared for their lethal activities by intracerebroventricular injection in mice (Fig. 3). All peptides were lethal in mice with characteristic symptoms of K^+ channel-acting toxins, such as tremor, convulsions, and spasmic paralysis followed by death. The following order of in vivo lethality was observed (from the most to the least potent peptide): OSK1 > AOSK1 > [Δ^1]-AOSK1 = [Δ^1,Thr^2]-AOSK1 > [Δ^{1-4}]-AOSK1 > [Δ^{1-6}]-AOSK1 > [Δ^{1-7}]-AOSK1 ≫ [Δ^{36-38}]-AOSK1. The greatest difference in lethality between AOSK1 and [Δ^{1-7}]-AOSK1, its N-terminal most truncated analog, is 6-fold. A good correlation seems to exist between the size of the N-terminal truncation of AOSK1 and the

TABLE 1

IC_{50} values of AOSK1 peptides on various K^+ channel subtypes

For each peptide, the IC_{50} value is provided in nanomolar concentration. Data for OSK1 are shown for comparison. No effects of the peptides were observed for Kv1.4, Kv1.5, Kv1.6, Kv1.7, Kv3.1, Kv11.1, $K_{Ca}1.1$, and $K_{Ca}2.1$ at micromolar concentrations. Specificity factors (the ratios between IC_{50} values for two channels) are shown for the sake of comparison.

	OSK1	AOSK1	[Δ^1]-AOSK1	[Δ^1,Thr^2]-AOSK1	[Δ^{1-4}]-AOSK1	[Δ^{1-6}]-AOSK1	[Δ^{1-7}]-AOSK1	[Δ^{36-38}]-AOSK1
LD_{50} (μg/kg)	2	2.5	3	3	5	6.5	15	40
IC_{50} (nM)								
Kv1.1	0.60 ± 0.04	0.40 ± 0.01	0.19 ± 0.01	0.36 ± 0.04	2.67 ± 0.50	2.18 ± 0.30	7.90 ± 1.20	365 ± 65
Kv1.2	5.40 ± 1.89	2.96 ± 0.01	30 ± 7	100 ± 5	245 ± 77	634 ± 5	N.E.	N.E.
Kv1.3	0.014 ± 0.001	0.003 ± 0.001	0.025 ± 0.002	0.021 ± 0.004	0.038 ± 0.001	0.045 ± 0.002	0.114 ± 0.005	1.85 ± 0.70
Kv3.2	N.E.	1000 ± 100	95 ± 10	65 ± 10	N.E.	N.E.	N.E.	N.E.
$K_{Ca}3.1$	225 ± 10	228 ± 92	425 ± 25	N.E.	N.E.	N.E.	N.E.	N.E.
Specificity factor								
Kv1.3 vs. Kv1.1	43	133	8	17	70	48	69	197
Kv1.3 vs. Kv1.2	386	987	1200	4762	6447	14089	N.D.	N.D.
Kv1.1 vs. Kv1.2	9	7	158	2778	92	291	N.D.	N.D.

N.E., no effects; N.D., not determined.

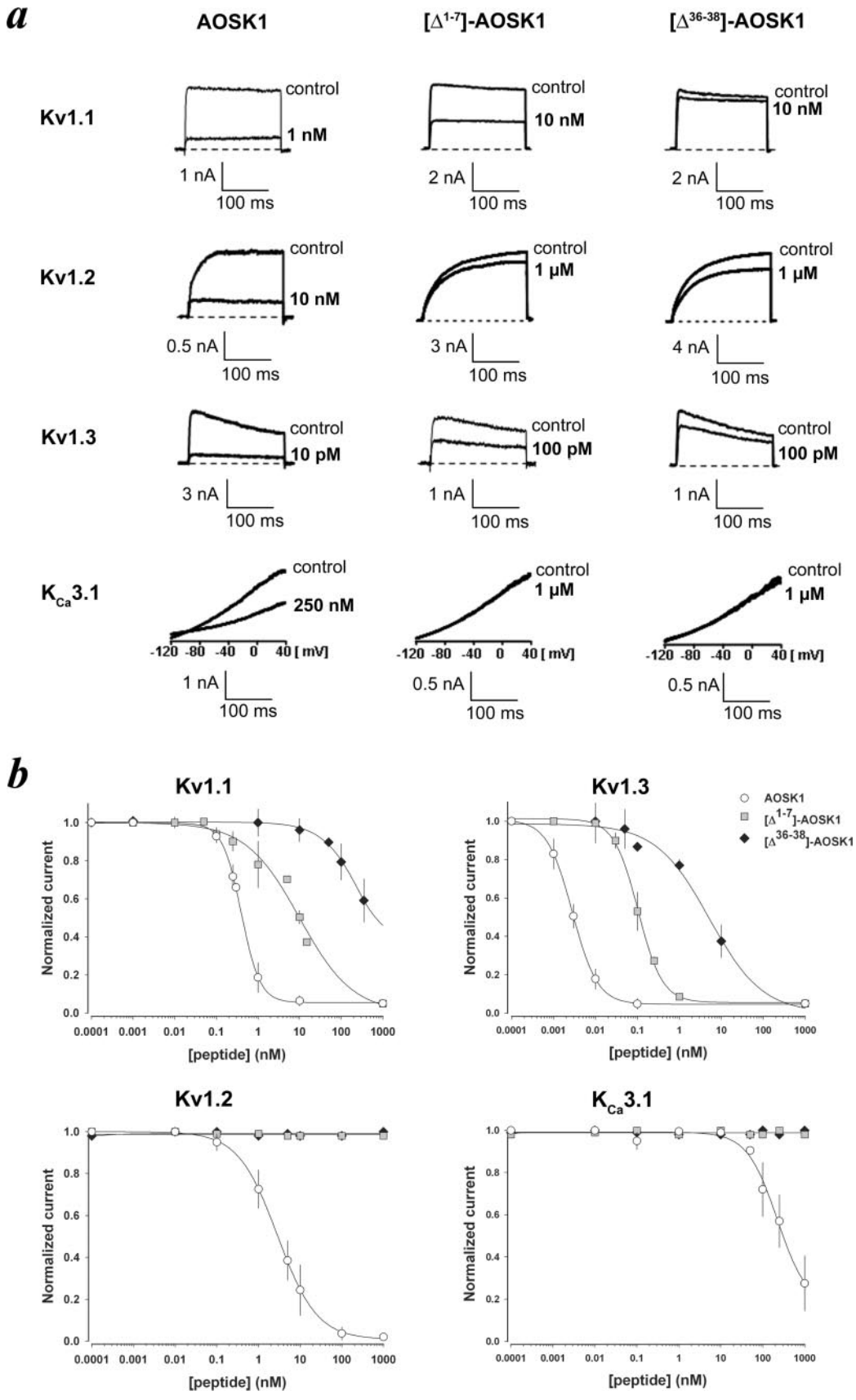

Fig. 4. Block of K^+ channel subtypes by AOSK1, N-terminal-truncated [Δ^{1-7}]-AOSK1, and C-terminal-truncated [Δ^{36-38}]-AOSK1. a, representative current traces in the absence (control) and presence (from left to right) of AOSK1, [Δ^{1-7}]-AOSK1 or [Δ^{36-38}]-AOSK1. The concentration of applied peptide is provided on the figure. From top to bottom: representative Kv1.1, Kv1.2, Kv1.3, and K_{Ca}3.1 potassium currents. b, average normalized current inhibition by various concentrations of AOSK1 (○), [Δ^{1-7}]-AOSK1 (▨), or [Δ^{36-38}]-AOSK1 (◆) for each channel type (Kv1.1, Kv1.2, Kv1.3, and K_{Ca}3.1 channels, as indicated). Each data point represents the mean value ± S.D. of four experiments.

resulting lethality of the AOSK1 peptides. This progressive decrease in lethality is believed to be associated with a decline in pharmacological potency toward vital K^+-channel subtype(s). In contrast, removal of the last three C-terminal AOSK1 residues (Thr^{36}, Pro^{37}, and Lys^{38}) dramatically reduced toxicity and increased the LD_{50} value 16-fold compared with AOSK1. Accordingly, a previous structural characterization of OSK1 (Jaravine et al., 1997) revealed that Thr^{36} side chain and Lys^{38} main chain mobility are important for the docking of OSK1 to K^+ channels.

Pharmacological Activity of AOSK1 Peptides on a Large Set of K^+-Channel Subtypes. The pharmacological profile of AOSK1 analogs was examined on 10 voltage-gated and 3 Ca^{2+}-activated K^+-channel subtypes. None of the newly synthesized peptides (OSK1, AOSK1, and its analogs) showed any activity on either the voltage-gated channels Kv1.4, Kv1.5, Kv1.6, Kv1.7, Kv3.1, and Kv11.1 or the Ca^{2+}-activated K^+ channels $K_{Ca}1.1$ and $K_{Ca}2.1$ at micromolar concentrations. In contrast, the peptides inhibited the Kv-1 family channels Kv1.1, Kv1.2, Kv1.3, the Kv3-family channel Kv3.2 and the intermediate-conductance Ca^{2+}-activated K^+ channel $K_{Ca}3.1$ with varying potencies (Table 1). As illustrated in Table 1 and Fig. 4, [Δ^{36-38}]-AOSK1 was the least effective of all analogs in blocking K^+-channel currents. This result agrees well with the observation that [Δ^{36-38}]-AOSK1 also shows the lowest activity when injected intracerebroventricular into mice (Fig. 3). However, [Δ^{36-38}]-AOSK1 low activity in vitro and in vivo was not unexpected because the integrity of the β-sheet structure has been reported to be crucial for the recognition of voltage-gated Kv and Ca^{2+}-activated $K_{Ca}3.1$ potassium channels by scorpion toxins (Castle et al., 2003; Rodriguez de la Vega et al., 2003; Jouirou et al., 2004; Regaya et al., 2004). In contrast, the most severe truncation of the N-terminal extended region of AOSK1 (i.e., [Δ^{1-7}]-AOSK1) produced differential effects depending on the subtype of K^+ channel (Fig. 4). AOSK1 activities on Kv1.1 and Kv1.3 currents were affected very little by the truncation of the last N-terminal seven residues in [Δ^{1-7}]-AOSK1 as shown in the dose-response curves in Fig. 4b. [Δ^{36-38}]-AOSK1 is shown for comparison. Whereas [Δ^{1-7}]-AOSK1's potency in blocking Kv1.1 (IC_{50} = 7.9 nM) and Kv1.3 (IC_{50} = 114 pM) decreased only 20- to 38-fold, it was completely inactive on Kv1.2 currents at 1 μM (Fig. 4), translating into a more than 338-fold loss in activity. Because the truncation of entire N-terminal extended domain of AOSK1 in [Δ^{1-7}]-AOSK1 showed such a differential effect on the affinity to Kv1.1, Kv1.2, and Kv1.3, we next examined whether milder truncations of this N-terminal domain could preserve the drastic reduction of activity on Kv1.2 while generating analogs with better affinities for Kv1.1 and Kv1.3. Figure 5 shows the effects of a progressive trimming of the N-terminal domain on the IC_{50} values of the resulting AOSK1 analogs. The data demonstrate that N-terminal domain trimming reduces the potency of the compounds to block Kv1.2 much more than their potency to block Kv1.1 and Kv1.3. This observation indicates the greater importance of the N-terminal extended domain for Kv1.2 channel recognition by AOSK1. The [Δ^1]-AOSK1 analog was of particular interest because it was 10- and 8-fold less potent on Kv1.2 and Kv1.3 but 2-fold more potent on Kv1.1 than AOSK1.

We further evaluated [Δ^1,Thr^2]-AOSK1 because its N-terminal domain is identical with the Kv1.3-blocking scorpion

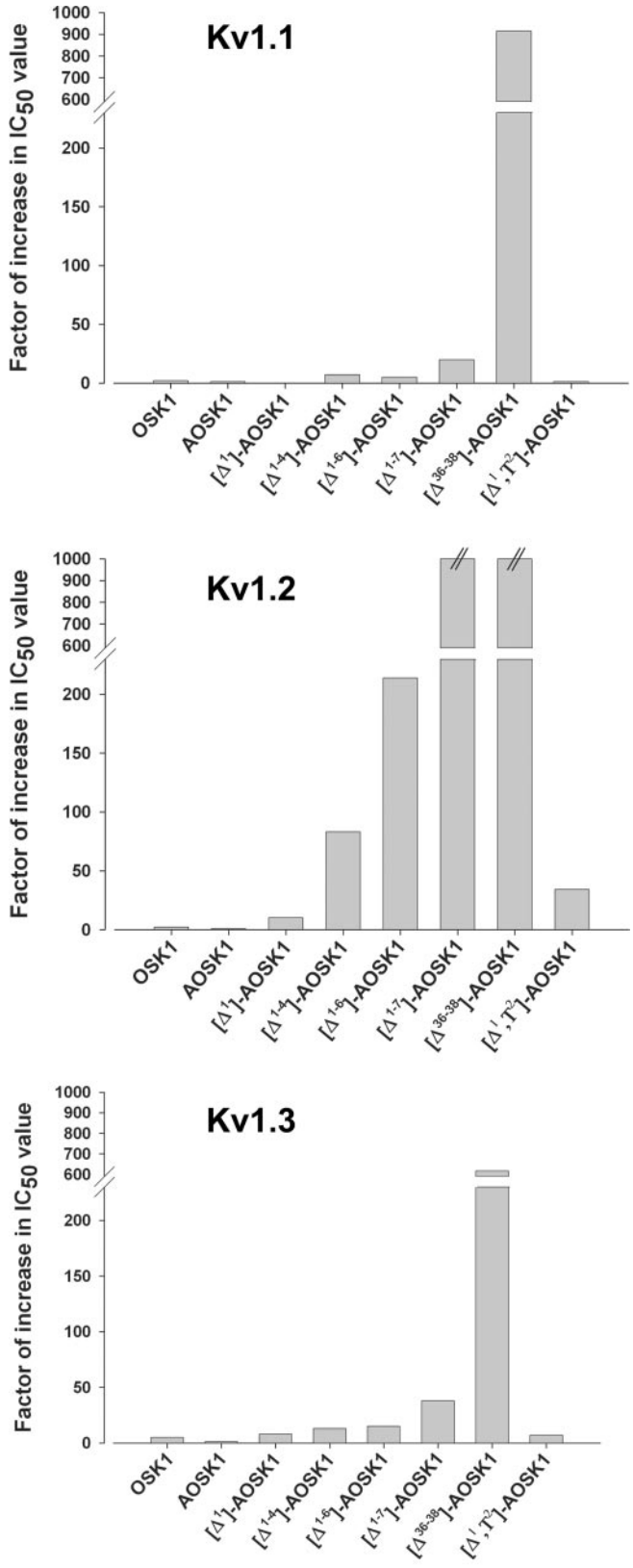

Fig. 5. Impact of N- and C-terminal truncations on blocking potencies of AOSK1 toward Kv1.1, Kv1.2, and Kv1.3 channels. AOSK1 versus its analogs: factors of increase in IC_{50} values for Kv1.1 (top), Kv1.2 (middle), and Kv1.3 channels (bottom). For each of these channel subtypes, the IC_{50} value of AOSK1 was normalized to 1 for the sake of comparison. The same scale was used for all three-channel types, illustrating the more drastic effects of truncations on Kv1.2 current blockage.

toxins [α-KTx2.1 (noxiustoxin) and α-KTx2.2 (margatoxin)] (Tytgat et al., 1999; Rodriguez de la Vega et al., 2003). [Δ^1,Thr^2]-AOSK1 was as potent as [Δ^1]-AOSK1 on Kv1.3, but its affinity further decreased by more than 3-fold for Kv1.2 compared with [Δ^1]-AOSK1 to finally give a 34-fold difference in affinity for this channel compared with AOSK1. As such, [Δ^1,Thr^2]-AOSK1 has a better selectivity than [Δ^1]-AOSK1 for Kv1.3. The N-terminal truncation strategy thus proves valuable for generating analogs with modified selectivity profiles and, possibly, with increased affinity toward specific channel subtype(s). Because AOSK1, but not OSK1, has a weak affinity for Kv3.2, we wondered whether any of the truncated AOSK1 analogs might be more potent Kv3.2 blockers than AOSK1. Figure 6 illustrates that two analogs, [Δ^1]-AOSK1 and [Δ^1,Thr^2]-AOSK1, are able to block Kv3.2 currents more potently than AOSK1. The increases in affinity were 11- and 15-fold for [Δ^1]-AOSK1 and [Δ^1,Thr^2]-AOSK1, respectively. Further truncations of AOSK1 had the opposite effect and resulted in a complete loss of activity on Kv3.2, which is in line with observations made for other voltage-gated K^+ channels (Fig. 4).

Comparison for each peptide between IC_{50} values on individual channels and LD_{50} values indicates an interesting trend worth discussing. In brief, it seems that the two most important channels for lethality in mouse brain are Kv1.1 and Kv1.2, as noticed previously (Mouhat et al., 2004b). It also seems that pharmacological activity on Kv3.2 is not essential for lethal potency. A tendency for a greater implication of Kv1.1 over Kv1.2 in the peptide-induced lethal effects is also evidenced. However, it should be noted that lethality probably involves other uncharacterized channels making such comparisons difficult.

Discussion

The scorpion toxin OSK1 serves as a good lead for the design of new Kv1.3 channel blockers because of its potent action on this channel type, with an IC_{50} value of 14 pM. OSK1's ability to also block other voltage-gated K^+ channels such as Kv1.1 and Kv1.2 (in the low nanomolar concentration range) and one Ca^{2+}-activated K^+ channel ($K_{Ca}3.1$) with moderate activity (at high nanomolar concentration) means that the toxin displays an unusual wide range of channel targets. AOSK1 is an even more interesting lead for further derivatization because it is one of the most potent Kv1.3 channel blockers described so far (Middleton et al., 2003; Mouhat et al., 2004b). Compared with other published compounds acting on Kv1.3, AOSK1 displays specificity factors of 133 (over Kv1.1; Table 1) and 987 (over Kv1.2), which thus seems to be similar to ShK-Dap^{22} (Kalman et al., 1998) but better than ShK-F6CA (Beeton et al., 2003) or ShK(L5) (Beeton et al., 2005). In addition, AOSK1 displays an even larger pharmacological profile through its additional action on Kv3.2. Therefore, AOSK1 is, to our knowledge, the second Kv3.2 channel blocker reported hitherto, after the sea anemone toxin ShK acting in the low nanomolar concentration range (Yan et al., 2005). Here, a strategy of domain trimming was used for the first time to generate new pharmacological profiles.

Several conclusions can be drawn from the experimental data obtained with these AOSK1 analogs. First, trimming in the C-terminal region of AOSK1 is expected to alter its β-sheet structure (Jaravine et al., 1997) and thereby reduces activity on all tested target channels. Second, trimming of the N-terminal region seems to be a more attractive strategy because the changes in activity differed greatly from one channel subtype to the other. Indeed, Kv1.1 and Kv1.3 channels were far less susceptible to decreases in analog affinity than was Kv1.2. It is interesting that a limited trimming of the AOSK1 N terminus turned out to be an interesting route for producing analogs with increased activity toward Kv3.2. We surmise that limited truncation may facilitate the access to the binding site of the peptides in the outer vestibule of the channel. As such, this indicates that some toxins can be inactive for a given channel type because of accessibility problems and perhaps not because they do not recognize a binding site on the channel. In future experiments, it will be interesting to combine various experimental strategies to obtain still more powerful toxin-derived drugs acting on specific voltage-gated and Ca^{2+}-activated potassium channels. In particular, structural determination and docking simulations of truncated AOSK1 peptides on the various target K^+ channels will be greatly helpful for this purpose. The challenge is to produce more selective AOSK1 analogs with high potencies on the Kv1.3 channel, with or without potent activity on $K_{Ca}3.1$ channel. In the end, such structure-function studies on AOSK1 may be useful for the production of potent

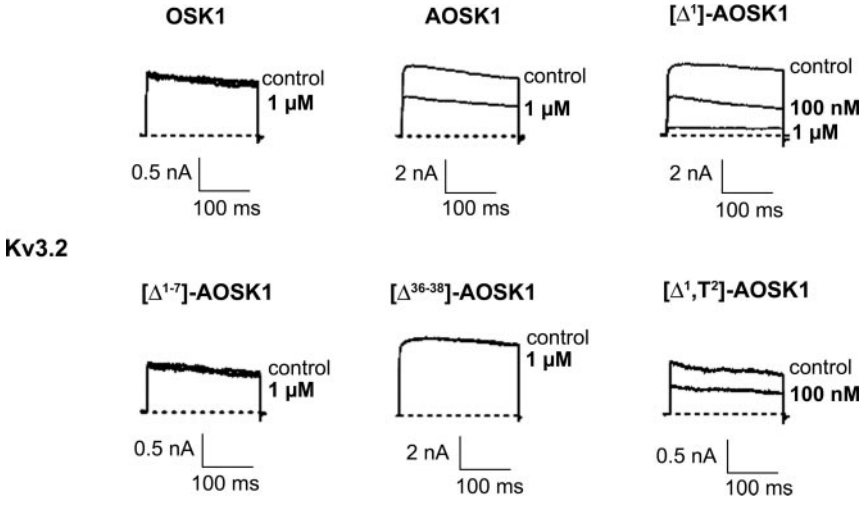

Fig. 6. Increased blocking potencies of [Δ^1]-AOSK1 and [Δ^1, Thr^2]-AOSK1 on Kv3.2 channel. Representative current traces in the absence (control) and presence of OSK1, AOSK1, [Δ^1]-AOSK1, [Δ^1,Thr^2]-AOSK1, [Δ^{1-7}]-AOSK1, or [Δ^{36-38}]-AOSK1. The concentration of applied peptide is provided for each. Note that OSK1 is inactive on Kv3.2 at micromolar concentration, contrary to AOSK1, and [Δ^1]-AOSK1 and [Δ^1,Thr^2]-AOSK1 are more potent than AOSK1 on Kv3.2 channel.

immunosuppressive drugs. Combining N-terminal truncations with point mutations is clearly a powerful way to create new selective toxin-derived peptide blockers for Kv1.3, Kv1.1, $K_{Ca}3.1$, and Kv3.2 channels.

Acknowledgments

We thank Dr. P. Mansuelle for Edman sequencing and amino acid analysis of AOSK1 peptides. Drs. B. De Rougé and E. Béraud are acknowledged for helpful discussions.

References

Aiyar J, Withka JM, Rizzi JP, Singleton DH, Andrews GC, Lin W, Boyd J, Hanson DC, Simon M, Dethlefs B, et al. (1995) Topology of the pore-region of a K^+ channel revealed by the NMR-derived structures of scorpion toxins. *Neuron* **15:**1169–1181.

Beeton C, Pennington MW, Wulff H, Singh S, Nugent D, Crossley G, Khaytin I, Calabresi PA, Chen CY, Gutman GA, et al. (2005) Targeting effector memory T cells with a selective peptide inhibitor of Kv1.3 channels for therapy of autoimmune diseases. *Mol Pharmacol* **67:**1369–1381.

Beeton C, Wulff H, Singh S, Botsko S, Crossley G, Gutman GA, Cahalan MD, Pennington M, and Chandy KG (2003) A novel fluorescent toxin to detect and investigate Kv1.3 channel up-regulation in chronically activated T lymphocytes. *J Biol Chem* **278:**9928–9937.

Bontems F, Roumestand C, Gilquin B, Ménez A, and Toma F (1991) Refined structure of charybdotoxin: common motifs in scorpion toxins and insect defensins. *Science (Wash DC)* **254:**1521–1523.

Castle NA, London DO, Creech C, Fajloun Z, Stocker JW, and Sabatier JM (2003) Maurotoxin: a potent inhibitor of intermediate conductance Ca^{2+}-activated potassium channels. *Mol Pharmacol* **63:**409–418.

Chandy KG, Wulff H, Beeton C, Pennington M, Gutman GA, and Cahalan MD (2004) K^+ channels as targets for specific immunomodulation. *Trends Pharmacol Sci* **25:**280–289.

Garcia ML, Garcia-Calvo M, Hidalgo P, Lee A, and MacKinnon R (1994) Purification and characterization of three inhibitors of voltage-dependent K^+ channels from *Leiurus quinquestriatus* var. *hebraeus* venom. *Biochemistry* **33:**6834–6839.

Grissmer S, Nguyen AN, Aiyar J, Hanson DC, Mather RJ, Gutman GA, Karmilowicz MJ, Auperin AA, and Chandy KG (1994) Pharmacological characterization of five cloned voltage-gated K^+ channels, types Kv1.1, 1.2, 1.3, 1.5 and 3.1, stably expressed in mammalian cell lines. *Mol Pharmacol* **45:**1227–1234.

Hamill OP, Marty A, Neher E, Sakmann B, and Sigworth FJ (1981) Improved patch-clamp techniques for high-resolution current recording from cells and cell-free membrane patches. *Pflueg Arch Eur J Physiol* **391:**85–100.

Jaravine VA, Nolde DE, Reibarkh MJ, Korolkova YV, Kozlov SA, Pluzhnikov KA, Grishin EV, and Arseniev AS (1997) Three-dimensional structure of toxin OSK1 from *Orthochirus scrobiculosus* scorpion venom. *Biochemistry* **36:**1223–1232.

Jouirou B, Mouhat S, Andreotti N, De Waard M, and Sabatier JM (2004) Toxin determinants required for interaction with voltage-gated K^+ channels. *Toxicon* **43:**909–914.

Kalman K, Pennington MW, Lanigan MD, Nguyen A, Rauer H, Mahnir V, Paschetto K, Kem WR, Grissmer S, Gutman GA, et al. (1998) ShK-Dap^{22}, a potent Kv1.3-specific immunosuppressive polypeptide. *J Biol Chem* **273:**32697–32707.

Merrifield B (1986) Solid phase synthesis. *Science (Wash DC)* **232:**341–347.

Middleton RE, Sanchez M, Linde AR, Bugianesi RM, Dai G, Felix JP, Koprak SL, Staruch MJ, Bruguera M, Cox R, et al. (2003) Substitution of a single residue in *Stichodactyla helianthus* peptide, ShK-Dap^{22}, reveals a novel pharmacological profile. *Biochemistry* **42:**13698–13707.

Mouhat S, Jouirou B, Mosbah A, De Waard M, and Sabatier JM (2004a) Diversity of folds in animal toxins acting on ion channels. *Biochem J* **378:**717–726.

Mouhat S, Visan V, Ananthakrishnan S, Wulff H, Andreotti N, Grissmer S, Darbon H, De Waard M, and Sabatier JM (2004b) K^+ channel types targeted by synthetic OSK1, a toxin from *Orthochirus scrobiculosus* scorpion venom. *Biochem J* **384:**1–10.

Possani LD, Selisko B, and Gurrola GB (1999) Animal toxins and potassium channels, in *Perspectives in Drug Discovery and Design* (Darbon H and Sabatier JM eds) vol 15/16, pp 15–40, Kluwer Academic Publishers, Dordrecht, The Netherlands.

Rauer H and Grissmer S (1996) Evidence for an internal phenylalkylamine action on the voltage-gated potassium channel Kv1.3. *Mol Pharmacol* **50:**1625–1634.

Regaya I, Beeton C, Ferrat G, Andreotti N, Darbon H, De Waard M, and Sabatier JM (2004) Evidence for domain-specific recognition of SK and Kv channels by MTX and HsTx1 scorpion toxins. *J Biol Chem* **279:**55690–55696.

Rodriguez de la Vega RC, Merino E, Becerril B, and Possani LD (2003) Novel interactions between K^+ channels and scorpion toxins. *Trends Pharmacol Sci* **24:**222–227.

Rodriguez de la Vega RC and Possani LD (2004) Current views on scorpion toxins specific for K^+-channels. *Toxicon* **43:**865–875.

Romi-Lebrun R, Lebrun B, Martin-Eauclaire MF, Ishiguro M, Escoubas P, Wu FQ, Hisada M, Pongs O, and Nakajima T (1997) Purification, characterization and synthesis of three novel toxins from the Chinese scorpion *Buthus martensi*, which act on K^+ channels. *Biochemistry* **36:**13473–13482.

Tytgat J, Chandy KG, Garcia ML, Gutman GA, Martin Eauclaire MF, van der Walt JJ, and Possani LD (1999) A unified nomenclature for short-chain peptides isolated from scorpion venoms: alpha-KTx molecular subfamilies. *Trends Physiol Sci* **20:**444–447.

Wulff H, Knaus HG, Pennington M, and Chandy KG (2004) K^+ channel expression during B cell differentiation: implications for immunomodulation and autoimmunity. *J Immunol* **173:**776–786.

Yan L, Herrington J, Goldberg E, Dulski PM, Bugianesi RM, Slaughter RS, Banerjee P, Brochu RM, Briest BT, Kaczorowski GJ, et al. (2005) *Stichodactyla helianthus* peptide, a pharmacological tool for studying Kv3.2 channels. *Mol Pharmacol* **67:**1513–1521.

Address correspondence to: Dr. Jean-Marc Sabatier, Centre National de la Recherche Scientifique Formation de Recherche en Evolution 2738, Boulevard Pierre Dramard, 13916 Marseille Cedex 20, France. E-mail: sabatier.jm@jean-roche.univ-mrs.fr